CrossMark

Ternary composites based on HDPE and Mater-Bi reinforced with hemp fibres

Study of the non-isothermal crystallization

C. J. Perez[1] · V. A. Alvarez[2]

Abstract The non-isothermal crystallization process of biodegradable thermoplastic matrix (Mater-Bi®, MB) and traditional thermoplastic (high-density polyethylene, polyethylene, PE) blends was studied using differential scanning calorimetry (DSC). Hemp fibres were used as filler, and maleic anhydride-functionalized high-density polyethylene (PE*) was employed as compatibilizer. SEM micrographs but also DSC studies show that MB forms immiscible blend with PE. The dispersed phase of molten MB acts as nucleating agent of PE enhancing the crystallization rate of PE, and also the solidified PE acts as nucleating agent by fastening the crystallization of MB. The values of half-time of crystallization ($t_{1/2}$) and the Z_c parameter from Avrami's method showed that for a fixed cooling rate, the crystallization rate decreased with the incorporation of hemp fibres and with the addition of the compatibilizer, PE*, showing the retarding effect of both components. Avrami's model was found to provide a fairly satisfactory description of the crystallization kinetics of the studied blends and composites. These results are further supported by the effective activation energy calculations obtained by applying the iso-conversional method of Friedman. CTT diagrams of studied materials were constructed, and they also reflected the effects of each component on the other one but also of hemp fibres and the compatibilizer.

Introduction

The development of conventional polymers, derived from fossil sources, has taken place since the first decades of the twentieth century, and because of its usefulness, the growth of the plastics industry has been very high, generating a massive consumption of it in many applications [1–5]. Due to waste accumulation at the end of life, the development of degradable polymeric materials, which are environmentally friendly, has become very important from the scientific and technological points of view [6, 7]. Biodegradable polymers constitute a family of new polymers planned to be degraded by living organisms giving an alternative to traditional non-degradable ones [6, 7]. Nevertheless, biodegradable polymers exhibit a great number of drawbacks that make them unsuitable for packaging applications, so other kind of strategies has to be taken into account. One of them is to combine a biodegradable polymer with a traditional one, for example a polyolefin, such as PE or PP. Because of their excellent processability and final properties, together with its low costs, polyolefin, and in particular polyethylene, has become a commodity; however, this polymer is non-biodegradable [8, 9]. One advantageous possibility is to develop blends of biodegradable polymers with traditional ones to obtain materials with improved cost/performances ratio, i.e. better higher mechanical properties together with low cost and intermediate biodegradation times [9–15].

✉ V. A. Alvarez
alvarezvera@fi.mdp.edu.ar

1 Polymer Science and Engineering Group, Research Institute of Material Science and Technology (INTEMA), National University of Mar del Plata (UNMdP), Av. Juan B. Justo 4302, 7600 Mar del Plata, Argentina

2 Composite Materials Group (CoMP), Research Institute of Material Science and Technology (INTEMA), National University of Mar del Plata (UNMdP), Solís 7575, 7600 Mar del Plata, Argentina

However, generally, the mechanical properties of these kinds of mixtures are not enough for the proposed application, and, in order to overcome such disadvantage, natural fibres can be incorporated to the mixtures [16]. It is known that this kind of fillers displayed a great number of advantages, such as, biodegradability, low cost and density, high specific properties and non-abrasive processing characteristics [17, 18]. In addition, the properties of polymeric matrix/natural fibres composites can be enhanced by applying chemical treatments to the fibres and/or to the polymers [19–21].

Within that field, Ul Haque et al. [16] have studied ternary systems: biodegradable polymer/conventional polymer/chemically treated hemp systems; however, no information about the crystallization behaviour of PE-based ternary systems is available in the literature.

It is known that the physical properties of polymer blends strongly depend on their crystallization behaviour and morphology. Particularly, when a two-system component is considered, one component crystallizes in the presence of the molten state of the other one, whereas the second component crystallizes in the presence of the solidified phase of the first one [22], due to the differences on the melting temperature of each polymer. So, studying the morphology and crystallization of both components is not only desirable but also necessary. Many articles have shown the effects of a second component on the crystallization behaviour of PE [23–26].

The aim of the present work was to study the non-isothermal crystallization behaviour of biodegradable polymer MB/PE blends and to analyse the effect of the incorporation of compatibilizer (maleic anhydride grafting PE) and natural fibres (hemp) on the analysed process. Most of the practical manufacturing techniques of polymer composites (polymer and reinforcement) involve crystallization conditions that are analogous to non-isothermal crystallization. The studied materials can be used mainly in packaging applications giving a balance between costs and properties; in addition, the knowledge of the crystallization behaviour is relevant in order to design the processing steps.

It is important to remark that we have published a previous work about dynamical crystallization of ternary composites based on polypropylene [27] as conventional polyolefin. The observed behaviour and also the obtained results were different from those obtained in the present work.

Materials and methods

Materials

A biodegradable and biocompostable thermoplastic, Mater-Bi® (MB), based on polycaprolactone (PCL), thermoplastic starch and additives (biodegradation time under controlled conditions: 20–45 days), with a degradation temperature around 420 °C, was kindly supplied by Novamont (Novara, Italy).

High-density polyethylene (PE), Eltex B5920 (MFR = 0.39 g/10 min), and high-density polyethylene-graft-maleic anhydride (PE*), Polybond 3009 (MFR = 3–6 g/10 min), were supplied by Solvay and Uniroyal Chemical, Italy, respectively.

Hemp (*cannabis sativa*) fibres were kindly supplied by Sassetti Agricoltura S.R.L. (Bientina, Italy). In order to remove the non-cellulosic components, the fibres were first washed with liquid soap and immersed in 6 mass% NaOH solution for 24 h at 40 °C. The alkali treatment increases the number of free hydroxyl groups on the fibre surface and produces changes in the chemical composition by extracting lignin and hemicellulose [28]. After NaOH treatment, the fibres were repeatedly rinsed with distilled water, dried at 105 °C and finally stored for use.

Preparation of blends and composites

Blends of MB with PE and their composites with hemp fibres (MB/PE/H) were prepared in a Brabender Plasticorder internal mixer at a temperature of 175 °C. The mixing was carried out under nitrogen flux for 7 min using a rotor speed of 60 rpm. To increase the compatibility of the components in the system, (PE*) copolymer was added (2 mass%) to composites.

The composites were prepared by using a two-step mixing procedure: In the first step, masterbatches of MB with NaOH-treated hemp (60/40 mass/mass) were processed in Brabender, and then in the second step, 80 mass% of masterbatch was melt-mixed with 20 mass% of polyolefin under the same conditions. In order to analyse the effect of compatibilizer on the morphology and final properties of blend and composite, 2 mass% of PE* was added to MB/PE matrix. All the examined systems are listed with their name in Table 1.

Scanning electron microscopy (SEM)

SEM analysis was carried out on the surfaces of samples cryogenically fractured in liquid nitrogen. The sample surfaces were sputter-coated with a fine layer of gold in an Edward Sputter Coater and analysed by a Jeol JSM-5600LV scanning electron microscope. The sizes of dispersed polyolefin phases in blends were measured with semi-automatic software (Image Pro-Plus) from SEM micrographs.

Non-isothermal crystallization process (differential scanning calorimetric tests)

Non-isothermal crystallization tests were carried out in a PerkinElmer Pyris 1 DSC. Pure indium was used as a

Table 1 Compositions and sample codes of examined materials

Sample name	Components	Compositions/mass%
MB	Mater-Bi	100
MB/PE	Mater-Bi/HDPE	70/30
MB/PE*	Mater-Bi/HDPE/HDPE-g-MAH	69/29/2
MB/PE/H	Mater-Bi/HDPE/Hemp	48/20/32
MB/(PE*)/H	Mater-Bi/HDPE/HDPE-g-MAH/Hemp	48/18/2/32
PE	HDPE	100

reference material to calibrate both the temperature scale and the melting enthalpy. All DSC runs were performed under nitrogen atmosphere. Samples of approximately 10.0 mg $\pm$ 0.1 mg were placed in aluminium pans and loaded at room temperature to the DSC, heated up rapidly to 200 °C and maintained at this temperature for 2 min to remove thermal history. Then, the non-isothermal crystallization studies were carried out by cooling the samples down to 20 °C at several cooling rates: 5, 10, 20 and 30 °C min^{-1}. Samples were tested in duplicate, and the average of both measurements was reported.

Theoretical background

Modelling of non-isothermal crystallization process

The relative degree of crystallinity as a function of temperature, $\alpha(T)$, can be calculated as [29, 30]:

$$\alpha(T) = \int_{T_o}^{T} ((\partial H_c/\partial T)dT) \Bigg/ \int_{T_o}^{T_\infty} ((\partial H_c/\partial t)dT) \tag{1}$$

where T_o and T_∞ represent the onset and final crystallization temperatures, respectively, and H_c is the crystallization enthalpy. Assuming that non-isothermal crystallization process may be composed by infinitesimally small isothermal crystallization steps, Ozawa [31] extended the Avrami's equation to the non-isothermal case as follows:

$$1 - \alpha = \exp(Z_t t^n) \tag{2}$$

where $K(T)$ is the function of cooling rate, φ is the cooling rate, and m is the Ozawa exponent depending on the crystal growth. Equation (2) can be transformed into:

$$\ln(-\ln(1-\alpha)) = \ln(K(T)) - m \times \ln \phi \tag{3}$$

By plotting $\ln(-\ln(1-\alpha))$ versus $\ln \phi$, at a given temperature, a straight line should be obtained, allowing to determine $K(T)$ and m.

This approach was applied to the early stages of crystallization, in order to avoid complications arisen from the effects of secondary crystallization process. Thus, relative crystallinity data in the range from 10 to 40 % were used.

It should be noted that n and Z_t ($K(T)$) in non-isothermal crystallization do not have the same physical significances as in the isothermal crystallization because, during non-isothermal crystallization, temperature is lowered constantly. Considering the non-isothermal character of the investigated process, Jeziorny [32] extended the isothermal Avrami's equation to the non-isothermal situation by proposing that the rate parameter, Z_t, should be corrected by cooling rate as follows:

$$\ln Z_c = \ln Z_t/\phi \tag{4}$$

where Z_c is the corrected kinetic rate constant.

A method developed by Mo can also be employed to describe the non-isothermal crystallization process of semi-crystalline polymers. Both Eqs. 3 and 4 can be related as follows:

$$\ln Z_t + n \ln t = \ln K(T) - m \ln \phi \tag{5}$$

By rearrangement at a given crystallinity α, the equation is converted into:

$$\ln \phi = \ln F(T) - a \ln t \tag{6}$$

where $F(T) = [K(T) \times Z_t - 1]1/m$ refers to the cooling rate, which must be chosen within unit crystallization time when the measured system amounts to a certain degree of crystallinity, and $a = n \times m - 1$ is the ratio between the Avrami's and the Ozawa's exponents.

As it was described above, the crystallization temperature depends on the cooling rate. For non-isothermal crystallization, it is interesting to evaluate the effective energy barrier for the process that can be obtained by applying the differential iso-conversional method of Friedman that uses the following equation [33]:

$$\ln(d\alpha/dt) = A - \Delta E_a/RT \tag{7}$$

where $d\alpha/dt$ is the crystallization rate for a given relative crystallinity, A is an arbitrary factor, and ΔE_a is the effective energy barrier of the process for a given relative conversion.

Thus, the relative crystallinity as a function of time, $\alpha(t)$, was differentiated to obtain the crystallization rate as a function of time. Then, by plotting $\ln (d\alpha/dt)$, measured at various cooling rate, against the corresponding inverse temperature for a given relative crystallinity, ΔE_a can be estimated from the slope.

It should be pointed out that evaluation of the activation energy presumes that the Arrhenius equation holds only within a region of the temperatures related to a given value of relative crystallization degree. Each of these regions is

much smaller than the complete non-isothermal crystallization temperature range (usually smaller than 10 °C). So, iso-conversional methods can be applied to non-isothermal crystallizations in order to evaluate the dependence of the effective activation energy on the relative crystallization degree and temperature [33].

Nucleation activity

Dobreva et al. [34] has developed an equation for calculating the nucleation activity (φ) of different substrates during the non-isothermal crystallization of polymer melts. If the reinforcement is extremely active, the nucleation activity will tend to zero, while for inert reinforcement, it will be close to one. For nucleation from the melt, the cooling rate is represented by Eq. (8) at temperatures close to melting:

$$\ln(\phi) = A - (B/\Delta T_c^2) \tag{8}$$

where ϕ is the cooling rate, A is a constant, $\Delta T_c = T_m - T_c$ is the degree of subcooling, T_c is the temperature corresponding to the peak temperature of DSC crystallization, T_m is the melting temperature, and B is a parameter related to the three-dimensional nucleation. The value of B for the pure polymer and its composites (B^*) was obtained from Eq. (8). Then, φ can be calculated by Eq. (9):

$$\varphi = B^*/B \tag{9}$$

Results and discussions

SEM micrographs of fracture surfaces of the examined blends (with and without compatibilizer) are presented in Fig. 1.

It can be observed that MB and dispersed polyolefin phase appear as separated phases, due to the immiscibility of components. MB/PE blends exhibited a characteristic droplet-like morphology with rather homogeneous size distribution. For MB/PE blends, the average size of dispersed phase was around 5 μm without any significant variation upon addition of 2 mass% PE*. SEM micrographs of fracture surfaces of composites with hemp showed weak interactions between matrix and fibres. On the other hand, the dispersion of fibres and polyolefin in the matrix appeared almost uniform. The addition of compatibilizer improved the adhesion between fibres and matrix, as a consequence of interactions between the anhydride groups and hydroxyl groups of polysaccharide chains (i.e. starch and cellulose). The occurrence of such interactions has been previously reported for several polyolefin composites compatibilized with maleated PE [35–37].

Differential scanning calorimetric tests

Figure 2 shows the crystallization behaviours of pure polymers and blends.

The values of crystallization temperature, extracted from the previous figure, are summarized in Table 2.

Curves show two crystallization peaks, which indicate that these blends have two crystallizable components: PE at higher temperatures (around 117 °C) and MB at lower temperatures (around 48 °C). For MB/PE blends, both MB and PE components were able to crystallize at the cooling rates employed in the study. PE crystallizes first, and the crystallization of MB occurred after complete crystallization of PE component. So, in the cooling conditions when PE component was crystallizing, MB component was in the molten state, and the crystallization of MB occurred in the presence of PE crystals. Thus, the crystallization of PE component could be affected by amorphous MB, and the crystallization behaviour of MB component could be influenced by the presence of crystals of PE component [38].
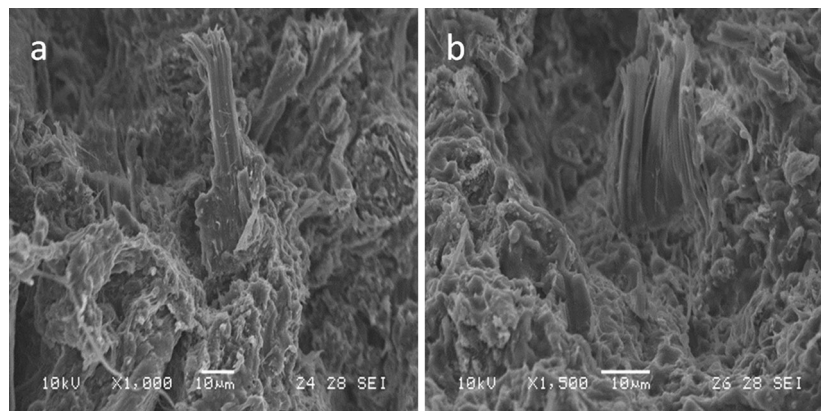

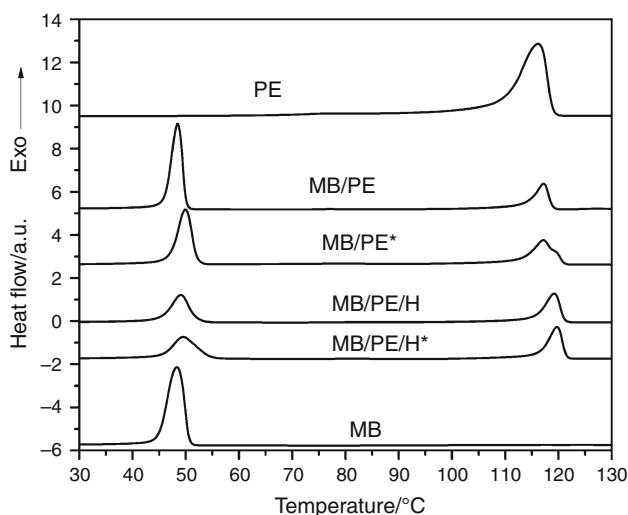**Fig. 1** Electronic micrographics by SEM for: **a** MB/PE/H and **b** MB/PE*/H

Fig. 2 Heat flow as a function of temperature at 10 °C/min for different samples during cooling

Table 2 Parameters of non-isothermal crystallization for different materials studied at 10/°C min^{-1}

System	$X^{MB}/\%$	$X^{PE}/\%$	$1/t_{1/2}^{MB}/s^{-1}$	$1/t_{1/2}^{PE}-/s^{-1}$
MB	64.4	–	0.028	–
MB/PE*/H	60.3	82.5	0.015	0.020
MB/PE/H	59.3	74.0	0.017	0.023
MB/PE*	62.2	61.0	0.019	0.016
MB/PE	71.7	43.3	0.050	0.030
PE	–	64.1	–	0.013

The degree of crystallinity of MB was around 65 % and clearly increased by PE incorporation, which in turn indicates that PE acts as nucleating agent for the crystallization of MB. The presence of hemp fibres decreased the crystallinity of MB. Similar values and tendency were found by other authors who have attributed that behaviour to the possibility that the fibres inhibit the crystallization process of the polymeric matrix [39–41].

However, the degree of crystallinity of PE shows a different behaviour in the MB/PE system and with the presence of hemp fibres. That parameter decreased in the MB/PE blend because during the PE crystallization, MB was in the molten (amorphous) state [39]. On the other hand, the addition of fibres increased the crystallinity of PE, and, in this case, the fibres act as nucleating agent [42–44].

The incorporation of PE* causes different behaviour in the crystallinity, producing a decrease in the crystallinity of MB and an increase in the crystallinity of PE in the MB/PE system. This could be associated with the reaction between the anhydride groups of the compatibilizer and the hydroxyl groups of starch present in MB [37].

The existence of both nucleating and retarding effects in the same blend may be due to that as mentioned previously, while PE crystallizes from the liquid, the other component, MB, crystallizes surrounded by a solid.

On the other hand, the presence of PE* and fibres produces a double effect: The addition of compatibilizer contributed to reducing the dispersed particle size of the polyolefin and improving the adhesion between fibre and matrix, as a consequence of interactions between the anhydride groups and hydroxyl groups of polysaccharide chains (i.e. starch and cellulose fibres) increasing, even more, the degree of crystallinity [44].

Figure 3 shows T_c^{MB}a and T_c^{PE}b as a function of cooling rate.

In both cases, T_c decreased as a function of cooling rate, because the nuclei became active at lower temperatures [45], conducting to smaller spherulites during the heterogeneous nucleation process. It is possible to observe that the crystallization temperature of PE (T_c^{PE}) increased with the incorporation of MB, indicating that the immiscible dispersed phase of MB acts as heterogeneous nuclei and PE starts to crystallize earlier, i.e. at a higher temperature [22]. Dissimilar behaviour was observed in the crystallization temperature of MB (T_c^{MB}), where MB was practically not affected by the presence of PE crystals. Furthermore, the incorporation of PE* showing different behaviour for T_c^{MB} and T_c^{PE}. T_c^{MB} increased notoriously (due to the interactions between the anhydride groups and hydroxyl group of starch), while T_c^{PE} slightly decreased because the low content of PE* seems not to affect the PE crystallization.

On the other hand, T_c^{PE} increased when hemp fibres were added to the MB/PE and MB/PE* systems, showing the nucleating effect, but T_c^{MB} shows a different behaviour. This parameter increased when hemp fibres were added to the MB/PE system, but decreased in the MB/PE* system. This can be attributed to the fact that the reaction produces branched chains and cross-linked macromolecules which have higher melt viscosity compared to linear macromolecules [37]. As it was previously mentioned, the addition of compatibilizer contributed to improving the adhesion between fibres and matrix, as a consequence of interactions between the anhydride groups and hydroxyl groups of polysaccharide chains.

Figure 4 shows overall crystallization rate as a function of cooling rate for (4a) MB crystallization and (4b) PE crystallization. A lower $t_{1/2}^{-1}$ value indicates slower crystallization. As it was expected, the value of OCR for MB and PE increased with the increase in the cooling rate for all materials. Table 2 also exhibits the obtained values at 10 °C min^{-1}. It can be observed that for a fixed cooling rate, the OCR of PE ($t_{1/2}^{PE-1}$) increased when MB is mixed
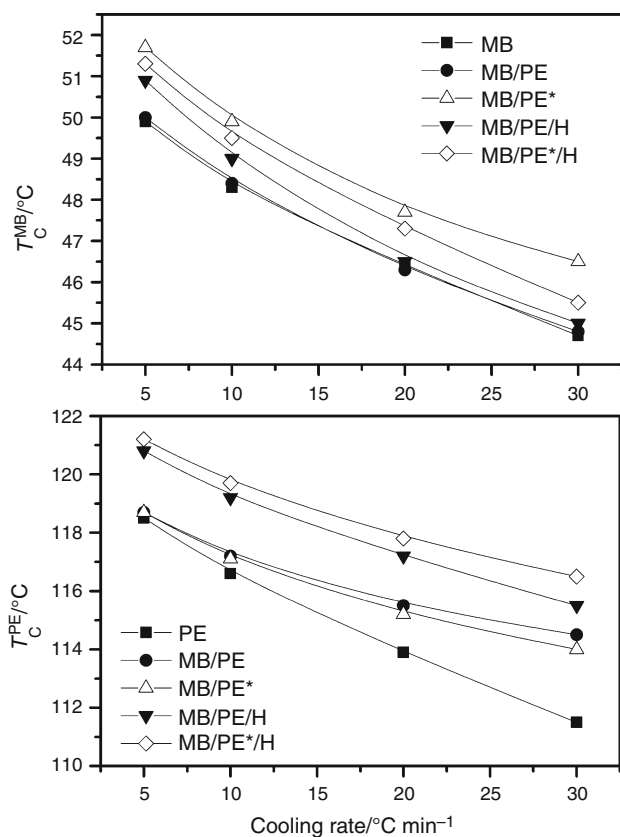
Fig. 3 T_c^{MB} (**a**) and T_c^{PE} (**b**) as a function of cooling rate

Fig. 4 Overall crystallization rate as a function of cooling rate for **a** MB crystallization and **b** PE crystallization

with PE, indicating that this component can accelerate the crystallization process, i.e. acts as nucleating effect. The same behaviour is observed in $t_{1/2}^{MB-1}$.

The use of PE* decreased the OCR of PE and MB in the MB/PE system, indicating a slower crystallization. This can be attributed to branched chains and cross-linked macromolecules which have higher melt viscosity compared to linear macromolecules produced during the reaction [37].

The OCR of MB in the PE/MB blends decreased with the addition of fibres and decreased further with the incorporation of PE*. The results showed that fibres played a dual role acting as both nucleating agents to promote nucleation and physical hindrances to retard the transport of chain segments during the non-isothermal crystallization process [46]. In addition, the OCR of PE also decreased with the fibres incorporation and the use of PE* retards the crystallization process, due to a better interaction of the fibres with maleic anhydride grafted in the PE [47].

Modelling of non-isothermal crystallization process

The parameters of Avrami model (Avrami exponent, n, and rate constant, Z_c) were calculated in the range of x between
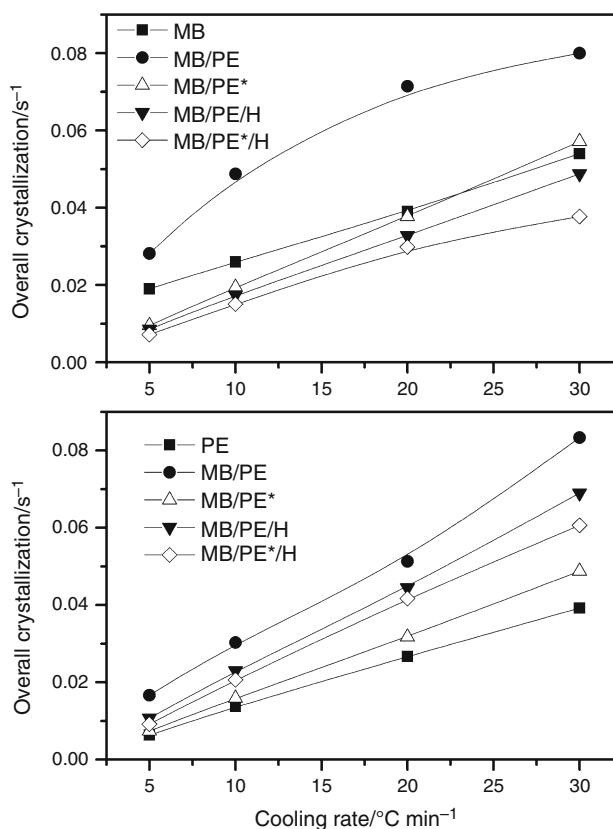
0.1 and 0.4, to avoid the problems that arise from the secondary crystallization [45]. The values of obtained n are summarized in Fig. 5, for the crystallization of MB and their blends (5a) and for the crystallization of PE and their blends (5b).

The pure matrices exhibited the lowest values. In all cases, in Fig. 5a, n decreased with the crystallization rate, while in the case of Fig. 5b, n was almost constant decreasing for the highest crystallization rate. Zou et al. [48] have reported that there are two factors which determine the value of n. One factor is that the fast crystallization rate of polymer at higher cooling rates prevents the spherulites from their full development, thereby lowering the value of n. Another one is that of growth site impingement, truncation of spherulites and secondary crystallization which may change the crystallization mechanism [48].

During the crystallization of MB, at a constant cooling rate (Fig. 5a), the variation in n value suggests that the fibres and the PE (alone and with PE*) exhibit different effects on the type of nucleation and crystal growth geometry. The average value of the Avrami exponent n for MB is close to 3 (at low cooling rate) which in turn indicates that the crystallization process involves heterogeneous nucleation with spherulitic type growth [45]. MB/PE
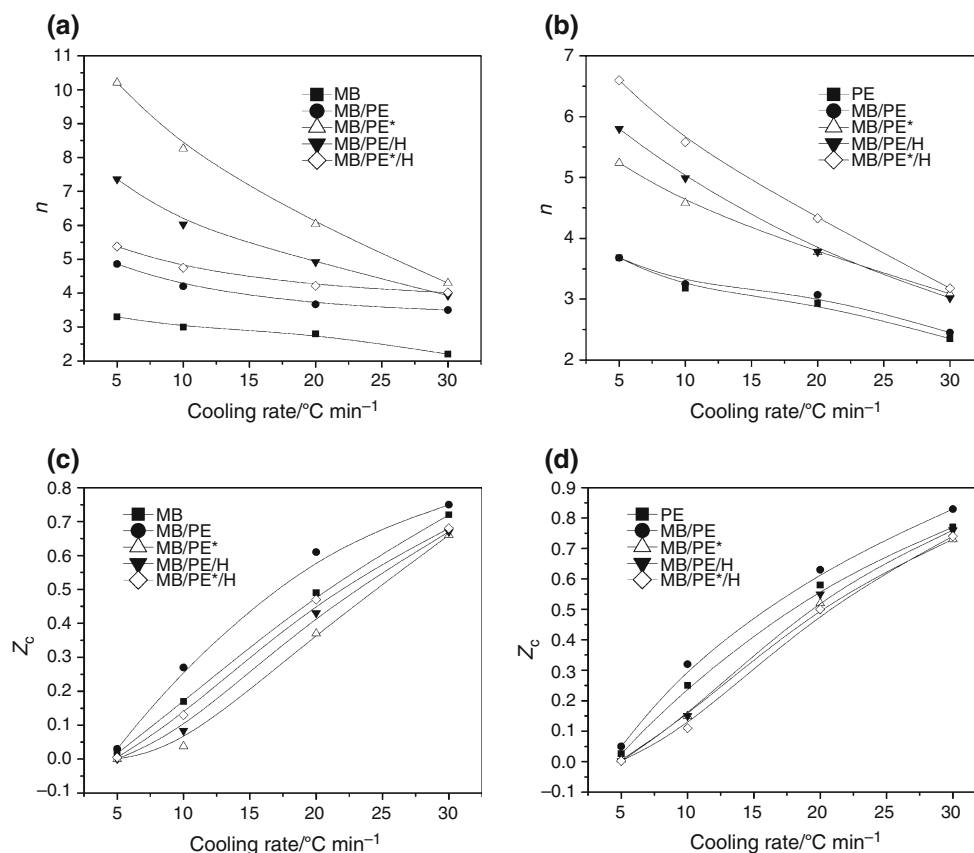
Fig. 5 Parameters of the Avrami's model (n, Z_c) as a function of the cooling rate for **a–c** MB crystallization in MB/PP blends and **b–d** PE crystallization in MB/PE blends

blend also presented n values close to 3, but it increased when the fibre is added to the material, indicating that it acts as nucleating agent and leads to three-dimensional spherulitic crystal growths [49]. As it was discussed earlier, the fibres retard the molecular mobility reducing the crystallization rate, but they could also be acting as nucleating agent to enhance the crystallization of MB [22]. On the other hand, at a constant cooling rate, the average value of n for the crystallization process of PE (Fig. 5b) is between 3.5 and 5.5 for neat PE and their blends with MB and H. The largest value of n in the MB/PE blend is attributed to great nucleating effect of MB, as it was previously mentioned. The Avrami exponent $n > 4$ indicates a more complicated nucleation type and spherulite growth form [50].

Figure 5c, d shows the corrected crystallization constant (Z_c) in function of cooling rate for MB and PP crystallization, respectively. In both figures, Z_c increased as a function of cooling rate, which is an expected behaviour because it is an indication of the crystallization rate getting faster as the cooling rate was increased [51, 52]. The crystallization rate of a polymer depends upon the nucleation mode, nucleation density and the growth rate of the

individual crystallites [49]. Z_c increases in the system MB/PE (nucleating effect of PE) and decreases with the fibres. Finally the MB/PE*/H system exhibited higher Z_c value than MB/PE/H one because PE* improves the system compatibility. Figure 5d shows that, at a given cooling rate, Z_c increased in the MB/PE system (by nucleating effect of MB) with respect to neat PE and decreased when the fibres were added, and finally it did not show important changes with the incorporation of PE*. All model results are in agreement with the experimental information discussed in previous section.

As it was described above, ΔE_a is the effective energy barrier of the process for a given relative conversion. ΔE_a was evaluated at a conversion of 0.3, and the values are reported in Table 3.

In both cases, for the crystallization of PE and MB, the activation energies increased when PE was mixed with MB, indicating the nucleating effect of each component (MB when PE crystallizes and PE when MB crystallizes), and this is in accordance with all previous results.

In the case of MB crystallization, ΔE_a increased when the fibres were added to the MB/PE and MB/PE* systems, and this is related to the physical hindrance of fibres to the

Table 3 Activation energy (ΔE_a) for the transport of the macromolecular segments to the growing surface at a conversion of 0.1, 0.3 and 0.5 and nucleation activity obtained by Dobreva method

	Nucleation activity	$-\Delta E_a/\text{kJ mol}^{-1}$		
		$X = 0.1$	$X = 0.3$	$X = 0.5$
MB crystallization				
MB	1.00	171	141	121
MB/PE	1.04	224	165	127
MB/PE*	0.98	246	166	134
MB/PE/H	0.95	229	171	153
MB/PE*/H	0.95	284	245	235
PE crystallization				
PE	1.00	303	275	463
MB/PE	1.11	417	346	402
MB/PE*	1.11	489	337	422
MB/PE/H	1.09	318	282	342
MB/PE*/H	1.09	219	202	335

motion of MB and PE chains, as it was previously mentioned. The relative high values of activation energy, found in the presence of hemp fibres in the MB/PE* system, could indicate a more ordered and organized structure of the transcrystalline layer compared with the bulk of the neat matrix as it was demonstrated in previous studies [53, 54].

On the other hand, the activation energy in the PE crystallization decreases when the fibres are added at both systems, indicating a more heterogeneous nucleation. The fibres dispersed increase the number of crystal nucleus per unit volume, leading to a decrease in ΔE_a [55].

Table 3 also shows calculated values of the nucleation activity. In the MB crystallization, the values are lower in the systems MB/PE/H and MB/PE*/H by the double-effect nucleating of PE and H, which is coincident with previous results. The effect is more notorious in the crystallization of PE, because MB presents a great nucleating effect during the crystallization of PE, but then decreased with the incorporation of fibres. The behaviour observed for the nucleation activity coincides with the evolution obtained with the *n* parameter from Avrami's equation.

Figure 6 shows the CCT, continuous cooling transformations where the crystallinity is related to time and temperature at a constant cooling rate.

This approach allows the knowledge of the crystallization process [56, 57]. The curves for a given relative degree of crystallinity (0.3) are plotted as a function of time. Each point on these curves has been obtained by integration of the full model (nucleation and growth) at constant cooling rate. So, when the degree of crystallization curve (for example by relative crystallinity at 0.3) is intercepted by a constant cooling rate one, the obtained point represents the time necessary to reach a specific relative degree of crystallization under specific thermal conditions. Figure 6a reveals that the
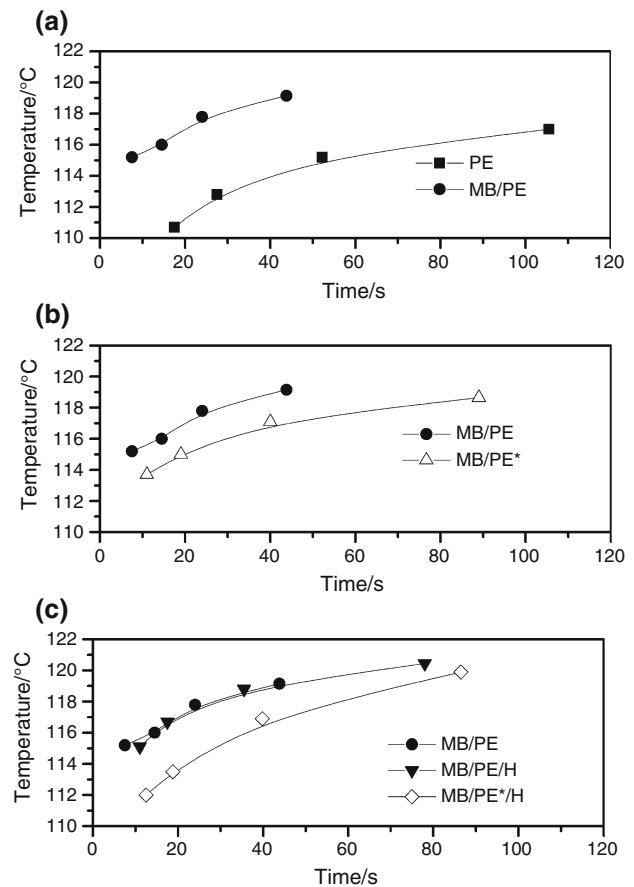
Fig. 6 CCT diagrams for PE crystallization for **a** PE and MB/PE, **b** PE and MB/PE/H, **c** MB/PE/H and MB/PE*/H

MB accelerates the crystallization process of PE (crystallized at higher temperature and in minor time), showing the nucleating effect observed previously. In the case of Fig. 6b, adding PE* to the MB/PE system retards the crystallization process (larger times and lower temperatures) with respect to the MB/PE system. Figure 6c shows the MB/PE/H and MB/PE*/H systems, indicating that the use of fibres retards the crystallization process and using PE* retards further the process. All results are in accordance with previous results. A similar (analogous) behaviour was observed in the CCT plots corresponding to the MB crystallization.

Conclusions

The non-isothermal crystallization of biodegradable thermoplastic matrix (Mater-Bi®) and traditional thermoplastic (polyethylene) blends was studied by means of DSC. Hemp fibres were used as filler, and maleic anhydride-functionalized polypropylene was employed as compatibilizer.

It was shown that the dispersed phases of molten MB act as nucleating agent to enhance the crystallization rate of PE and the solidified PE acted as nucleating agent to enhance

the crystallization of MB. All experimental and model parameter results indicate that fibres retarded the crystallization process, whereas the PE* produces counteracting effects.

The full model was used in order to build the CCT diagrams. These diagrams allow the determination of the crystallinity degree for different processing conditions. This information is very useful for the design and optimization of processing step. Besides, these diagrams confirmed the nucleating and retarding effects of different components in accordance with all previous analysis.

The calculation of the nucleation activity of the component, based on data from non- isothermal crystallization tests on cooling from the melt various rates, proved that in the MB crystallization, the values are lower in the systems MB/PE/H and MB/PE*/H by the double-effect nucleation of PE and H. On the other hand, in the crystallization of PE, MB displayed a great nucleating effect during the crystallization of PE, but then decreased with the incorporation of natural fibres.

References

1. Meneses J, Corrales CM, Valencia M. Synthesis and characterization of biodegradable polymers from cassava starch (in Spanish). Revista EIA. 2007;8:57–67.
2. Mulder KF. Sustainable consumption and production of plastics? Technol Forecast Soc. 1998;58:105–24.
3. Mutha NH, Patel M, Premnath V. Plastics materials flow analysis for India. Resour Conserv Recy. 2006;47:222–44.
4. Dikgang J, Leiman A, Visser M. Analysis of the plastic-bag levy in South Africa. Resour Conserv Recycl. 2012;66:59–65.
5. Biron M. The plastics industry: economic overview. Thermoplastics and thermoplastic composites. 2nd Revised edition. USA: William Andrew Publishing; 2012. p. 31–131.
6. Bastioli C. Biodegradable materials. In: Brody AL, Marsh KS, editors. The Wiley encyclopedia of packaging technology. 2nd ed. London: Wiley; 1987. p. 77–83.
7. Bastioli C, Biodegradable materials state of art and future perspectives. Frontiers in the science and technology of the polymer recycling. Antalya, Turkey; 1997.
8. Siracusa V, Rocculi P, Romani S, Dalla Rosa M. Biodegradable polymers for food packaging: a review. Trends Food Sci Tech. 2008;19:634–43.
9. Arcana M, Bundjali B, Yudistira I, Jariah B, Sukria L. Study on properties of polymer blends from polypropylene with polycaprolactone and their biodegradability. Polym J. 2007;39:1337–44.
10. Clarinval AM, Halleux J. Biodegradable polymers for industrial applications, R. Smith, editor. Chapter 1. Elsevier Editorial; 2000. pp 1–29.
11. Pimentel TAPF, Durâes JA, Drummond AL, Schlemmer D, Falcão R, Araújo Sales MJ. Preparation and characterization of blends of recycled polystyrene with cassava starch. J Mater Sci. 2007;42:7530–6.
12. Schlemmer D, De Oliveira ER, Araújo Sales MJ. Polystyrene/thermoplastic starch blends with different plasticizers. J Therm Anal Calorim. 2007;87:635–8.
13. Schlemmer D, Araújo Sales MJ, Resck IS. Degradation of different polystyrene/thermoplastic starch blends buried in soil. Carbohyd Polym. 2009;75:58–62.
14. Kiatkamjornwong S, Sonsuk M, Wittayapichet S, Prasassarakich P, Vejjanukroh PC. Degradation of styrene-g-cassava starch filled polystyrene plastics. Polym Degrad Stabil. 1999;66:323–35.
15. Kaewtip K, Tanrattanakul V. Preparation of cassava starch grafted with Polystyrene by suspension Polymerization. Carbohyd Polym. 2008;73:647–55.
16. Haque MM, Alvarez V, Paci M, Pracella M. Processing, compatibilization and properties of ternary composites of Mater-Bi with polyolefins and hemp fibres. Compos Part A Appl Sci. 2011;42:2060–9.
17. Pracella M, Pancrazi C, Haque MM, D'Alessio A. Thermal and microstructural; characterization of compatibilized polystyrene/natural fillers composites. J Therm Anal Calorim. 2011;103:95–101.
18. Pracella M, Haque MM, Alvarez V. Functionalization, compatibilization and properties of polyolefin composites with natural fibres. Polymers. 2010;2:554–74.
19. Mwaikambo LY, Ansell MP. Chemical modification of hemp, sisal, jute, and kapok fibres by alkalization. J Appl Polym Sci. 2002;84:2222–34.
20. Pracella M, Chionna D, Kulinski Z, Piorkowska E. Functionalization, compatibilization and properties of polypropylene composites with hemp fibres. Compos Sci Technol. 2006;66:2218–30.
21. Alvarez V, Mondragón I, Vázquez A. Influence of chemical treatments on the interfacial adhesion between sisal fibre and different biodegradable polymers. Compos Interface. 2007;14:605–16.
22. Huang JW, Wen YL, Kang CC, Yeh MY, Wen SB. Morphology, melting behavior, and non-isothermal crystallization of poly(butylene terephthalate)/poly(ethylene-co-methacrylic acid) blends. Termochim Acta. 2007;465:48–58.
23. Wenig W, Meyer K. Investigation of the crystallization behaviour of polypropylene—polyethylene blends by optical microscopy. Colloid Polym Sci. 1980;258:1009–14.
24. Li J, Shanks RA, Long Y. Miscibility and crystallization of metallocene polyethylene blends with polypropylene. J Appl Polym Sci. 2003;87:1179–89.
25. Li J, Shanks RA, Long Y. Time dependent morphology of polyethylene-polypropylene blends. Chin J Polym Sci. 2002;20:497–508.
26. Sweed M. Co-crystallization in polyolefins blends studied by various crystallization analysis techniques. Thesis MSC (Chemistry and Polymer Science), Stellenbosch University, South Africa; 2006.
27. Perez CJ, Alvarez V. Non isothermal crystallization of biodegradable polymer (MaterBi)/polyolefin (PP)/Hemp fibres ternary composites. J Therm Anal Calorim. 2015;120:1445–55.
28. Alvarez V, Ruseckaite R, Vazquez A. Mechanical properties and water absorption behavior of composites made from a biodegradable matrix and alkaline-treated sisal fibres. J Compos Mater. 2003;37:1575–88.
29. Yam WY, Ismail J, Kammer HW, Schmidt H, Kummerlöwe C. Polymer blends of poly(ε-caprolactone) and poly(vinyl methyl ether)—thermal properties and morphology. Polymer. 1999;40:5545–52.
30. Lin CC. The rate of crystallization of poly(ethylene terephthalate) by differential scanning calorimetry. Polym Eng Sci. 1983;23:113–6.
31. Avrami M. Kinetics of phase change. II Transformation-time relations for random distribution of nuclei. J Chem Phys. 1940;8:212–6.
32. Jeziorny A. Parameters characterization the kinetics of the non Parameters characterizing the kinetics of the non-isothermal

crystallization of poly(ethylene terephthalate) determined by d.s.c. Polymer. 1978;19:1142–4.

33. Vyazovkin S, Sbirrazzuoli N. Isoconversional analysis of calorimetric data on nonisothermal crystallization of a polymer melt. J Phys Chem B. 2003;107:882–8.

34. Dobreva A, Gutzow I. Activity of substrates in the catalyzed nucleation of glass-forming melts. II. Experimental evidence. J Non-Cryst Solids. 1993;162:13–25.

35. Feng D, Caulfiled DF, Sanadi AR. Effect of compatibilizer on the structure property relationships of kenaf fibre/polypropylene composites. Polym Compos. 2001;22:506–17.

36. Doan TTL, Gao SL, Mader E. Jute/polypropylene composites I. Effect of matrix modification. Compos Sci Technol. 2006;66:952–63.

37. Majid RA, Ismail H, Taib RM. Effects of polyethylene-g-maleic anhydride on properties of low density polyethylene/thermoplastic sago starch reinforced kenaf fibre composites. Iran Polym J. 2010;19:501–10.

38. He YS, Zeng JB, Li SL, Wang YZ. Crystallization behavior of partially miscible biodegradable poly(butylene succinate)/poly(ethylene succinate) blends. Termochim Acta. 2012;529:80–6.

39. Akos IN, Wyasu G, Ladan Z. Effect of fibre load and compatibilization on biodegradation of poly(ε-caprolactone)/poly(lactic acid) composites. Int Res J Mat Sci Eng. 2014;1:2–11.

40. Abdelmouleh M, Boufi S, Belgacem MN, Dufresne A. Short natural-fibre reinforced polyethylene and natural rubber composites: effect of silane coupling agents and fibres loading. Compos Sci Technol. 2007;67:1627–39.

41. Campos A, Marconcini JM, Imam SH, Klamczynski A, Ortis WJ, Wood DH, WilliamsTG Martins-Franchetti SM, Mattoso LHC. Morphological, mechanical properties and biodegradability of biocomposite thermoplastic starch and polycaprolactone reinforced with sisal fibres. J Reinf Plast Comp. 2012;31:573–81.

42. Puglia D, Kenny JM, Santulli C, Sarasini F, Valente T. Thermal and mechanical characterization of phormium tenax reinforced polypropylene composites. J Thermoplast Compos. 2014;27:1493–503.

43. Barone JR. Polyethylene/keratin fibre composites with varying polyethylene crystallinity. Compos Part A Appl Sci. 2005;36:1518–24.

44. Sailaja RRN, Deepthi MV. Mechanical and thermal properties of compatibilized composites of polyethylene and esterified lignin. Mat Design. 2010;31:4369–79.

45. Di Lorenzo ML, Silvestre C. Non-isothermal crystallization of polymers. Prog Polym Sci. 1999;24:917–50.

46. Bin T, Qu J, Liu L, Feng Y, Hu S, Yin X. Non-isothermal crystallization kinetics and dynamic mechanical thermal properties of poly(butylene succinate) composites reinforced with cotton stalk bast fibres. Thermochim Acta. 2011;525:141–9.

47. Bouza R, Marco C, Ellis G, Martín Z, Gómez MA, Barral L. Analysis of the isothermal crystallization of polypropylene/wood flour composites. J Therm Anal Calorim. 2008;94:119–27.

48. Zou P, Tang S, Fu Z, Xiong H. Isothermal and non-isothermal crystallization kinetics of modified rape straw flour/high-density polyethylene composites. Int J Therm Sci. 2009;48:837–46.

49. Deshmukh GS, Peshwe DR, Pathak SU, Ekhe JD. Nonisothermal crystallization kinetics and melting behavior of poly(butylene terephthalate) (PBT) composites based on different types of functional fillers. Thermochim Acta. 2014;581:41–53.

50. Saengsuwan S, Tongkasee P, Sudyoadsuk T, Promarak V, Keawin T, Jungsuttiwon S. Non-isothermal crystallization kinetics and thermal stability of the in situ reinforcing composite films based on thermotropic liquid crystalline polymer and polypropylene. J Therm Anal Calorim. 2011;103:1017–26.

51. Alvarez V, Perez CJ. Gamma irradiated LDPE in presence of oxygen. Part I. Non-isothermal crystallization. Thermochim Acta. 2013;570:64–73.

52. Perez CJ, Alvarez V. Overall crystallization behavior of polypropylene-clay nanocomposites; Effect of clay content and Polymer/clay compatibility on the bulk crystallization and spherulitic growth. J Appl Polym Sci. 2009;114:3248–60.

53. Klein N, Selivansky D, Marom G. The effects of a nucleating agent and of fibres on the crystallization of nylon 66 matrices. Polym Compos. 1995;16:189–96.

54. Buzarovska A, Bogoeva-Gaceva G, Grozdanov A, Avella M, Gentile G, Errico M. Crystallization behavior of poly(hydroxy-bytyrate-co-valerate) in model and bulk PHBV/kenaf fibre composites. J Mater Sci. 2007;42:6501–9.

55. Wang H, Chu H, Ding M, Min S, Jiang S, Shaotong J. Crystallization behavior of bamboo shoot shell/high-density polyethylene composites. J Reinf Plast Comp. 2012;31:405–13.

56. Pruiell J, White J. Structure development during polymer processing: studies of the melt spinning of polyethylene and polypropylene fibres. Polym Eng Sci. 1975;15:660–7.

57. Hsiung C, Cakmak M, White J. Structural gradients in injection molded poly-*p*- phenylene sulfide: influence of processing conditions and effect on mechanical behavior. Int Polym Proc. 1990;5:109–16.